RSC Advances

PAPER

View Article Online
View Journal | View Issue



Cite this: *RSC Adv.*, 2024, **14**, 1009

# Preparation of multifunctional ceramic foams for sound absorption, waterproofing, and antibacterial applications†

Xizhi Zhang,[a] Xiaozhong Chen,[b] Wenchao Min,[c] Guowei Liang,[d] Wei Zhang,[a] Shuheng Yao[a] and Ximing Zhong *[b]

Using porous materials for sound absorption is an effective approach to alleviating noise pollution, although their hydrophilic properties potentially cause concerns regarding public safety and health risks. This work provides a facile strategy for establishing a multifunctional ceramic system by using sponges as the sintering template, adjusting the pore structure of ceramic foams by varying the ceramic slurry weights and fluorinating the sintered ceramic foams *via* hydrolysis and condensation processes to provide low surface energy. The obtained porous ceramic foams demonstrate sound-absorbing, waterproof, and antibacterial properties. The results reveal that the increase in ceramic slurry weight decreases the pore size and porosity due to the formation of more compact structures, and the decrease in porosity compromises the sound absorption performance. In the middle-range sound frequency, the maximum sound absorption coefficient reached 0.92. In addition, the fluorination of the rough ceramic surfaces endows the ceramic foams with waterproof properties, which enables them to float on water and display the silver mirror phenomenon. In addition, due to the waterproof property reducing the contact area between the ceramic surface and the bacterial suspension, as well as the lipophilic fluorine chain disrupting the bacterial structures, these ceramic foams exhibited antibacterial rates above 95%. In addition, the mechanisms underlying the sound-absorbing, waterproof, and antibacterial properties of these porous ceramic foams are elucidated. Therefore, this work provides a facile approach to developing a multifunctional ceramic system. Their practical features make these ceramic foams more significant in the field of noise reduction.

Received 1st October 2023
Accepted 11th December 2023

DOI: 10.1039/d3ra06675d

rsc.li/rsc-advances



## 1. Introduction

The rapid development of urbanization and industrialization gives rise to severe environmental and social problems associated with noise pollution, which critically aggravates the quality of life and human health, causing hearing disorders, sleep disorders, and mental disorders.[1–3] To alleviate the growing noise pollution, appropriate approaches are sought. Many researchers have revealed that porous materials are attractive candidates for achieving noise reduction.[4,5] Due to the high surface areas of porous materials, incident sound waves are converted to heat, which then dissipates *via* friction with the pore walls, and the sound energy can also be consumed through the resonance of the pore walls and the process of energy transformation.[6] Generally, porous organic, metallic, and inorganic nonmetallic materials are widely applied in sound absorption because they possess the advantages of light weight, high surface area, and easy shaping.[7]

As for porous organic materials, polyurethane and polyvinyl chloride, for instance, although they exhibit the merits of low cost and simple preparation, their disadvantages, such as low thermal stability and weathering resistance, limit their long-term applications.[8–11] Filip *et al.* prepared nanofibrous mats by electrospinning blends of virgin and recycled poly(vinyl butyral), and these organic systems exhibited good sound-adsorbing performance.[12] Porous metallic materials, such as copper and aluminum, generally demonstrate the advantages of high temperature resistance and fire retardancy, while they exhibit the limitation of low chemical stability.[13,14] By improving the morphological parameters, Jafari *et al.* obtained a porous aluminum metal foam with a high absorption coefficient at the desired frequency.[15] Porous inorganic nonmetallic materials, such as ceramic foams, eliminate the shortcomings of organic

[a]*Faculty of Humanities and Arts, Macau University of Science and Technology, Taipa, Macau 999078, China*

[b]*School of Chemistry and Chemical Engineering, Zhongkai University of Agriculture and Engineering, Guangzhou, Guangdong 510225, China. E-mail: zhongximing2006@126.com*

[c]*HeXiangNing College of Art and Design, Zhongkai University of Agriculture and Engineering, Guangzhou, Guangdong 510225, China*

[d]*School of Materials Science and Engineering, South China University of Technology, Guangzhou, Guangdong 510641, China*

† Electronic supplementary information (ESI) available. See DOI: https://doi.org/10.1039/d3ra06675d

and metallic materials and demonstrate unique advantages, such as good thermal and chemical stability, which make them ideal candidates for sound reduction in crucial environments.[16–18] For example, Du *et al.* investigated the effect of structural factors on the sound absorption properties of silicon nitride ceramic foams and the results revealed that higher porosity and smaller pore size were conducive to better sound absorption by these ceramic foams.[7] They could withstand a sintering temperature of 1700 °C, indicating that such ceramic foams could be used in critically high temperatures.

To achieve better sound-absorbing performance, combining the features of different materials is an intriguing approach.[19–22] Lin *et al.* used hollow ceramic microspheres as the filler in polyurethane foam to strengthen the mechanical properties of their composites, and these composites exhibited synergistic sound absorption properties derived from the sound absorption efficacy of the polyurethane pores and the hollow attribute of the ceramic microspheres.[23] Multifunctional sound-absorbing materials are more attractive and useful. Bao *et al.* employed a combination of structural engineering and polymer-protection strategy to develop hierarchical Fe/C hollow microspheres by the assembly of centripetal Fe/C nanosheets, and the obtained hollow composite exhibited an effective integration of sound absorption and microwave absorption.[24] Zhao *et al.* established a scalable high-porosity wood system using a rapid high-temperature process followed by ambient drying, and this system demonstrated extraordinary sound absorption and thermal insulation.[25] Notably, although good sound-absorbing performance was achieved, the adverse effects derived from hydrophilicity could not be ignored. As for outdoor-use sound-absorbing materials, due to hydrophilicity, the rapid absorption of water on rainy days inevitably brings about a significant increase in weight, causing tremendous pressure on the substrates and potential risks to human safety. In addition, the wet environment is conducive to bacterial proliferation, which may pose a threat to public health. Therefore, it is highly desirable to establish a waterproof sound-absorbing system that can not only achieve noise reduction but also ensure public safety.

Furthermore, to provide materials with waterproof properties, the grafting of polydimethylsiloxane (PDMS) or fluorine-containing chains is generally adopted because of their low surface energy.[26–31] Notably, fluorine-containing compounds generally possess a lower surface energy than PDMS, indicating a better waterproof performance. In addition, previous reports have revealed that various liquids can slide off on fluorine-modified rough surfaces, whereas, oily liquids would compromise the waterproof property of PDMS-modified rough surfaces, suggesting that fluorine-modified porous materials are more suitable for applications in harsh conditions.[32,33] In addition, fluorine-containing compounds have been proven to demonstrate antibacterial performance by disrupting the bacterial structure.[34,35] Therefore, it is possible to establish a sound-absorbing system with superior waterproof and antibacterial properties.

In this work, to develop porous ceramic foams with sound-absorbing, waterproof, and antibacterial properties, sponges were used as the sintering template, and the weight of the ceramic slurry (mainly consisting of $SiO_2$, $Al_2O_3$, $K_2O$, and $Na_2O$) was varied to obtain different pore structures. Furthermore, 1*H*,1*H*,2*H*,2*H*-perfluorodecyltrimethoxysilane (PFDTMS) was employed to coat the rough sintered ceramic surfaces *via* hydrolysis and condensation to provide low surface energy. The ceramic components were verified using various characterization techniques, and the pore structures were confirmed by SEM. The results reveal that the increase in ceramic slurry resulted in a decrease in pore size and porosity, and the collaboration of the above two factors resulted in better sound absorption properties. In addition, high water contact angles were achieved on the fluorinated ceramic surfaces, and these ceramic foams could even float on water instead of sinking, indicating their remarkable waterproof properties. In addition, owing to the fluorination treatment, the obtained ceramic foams demonstrated outstanding antibacterial performance, and the antibacterial rates were above 95%. Therefore, these porous ceramic foams demonstrate sound-absorbing, waterproof, and antibacterial performance, and such multifunctional properties make them good candidates for practical applications.

## 2. Experimental section

### 2.1. Materials

Acetic acid and hexane were provided by Aladdin. 1*H*,1*H*,2*H*,2*H*-Perfluorodecyltrimethoxysilane (PFDTMS) was purchased from Macklin, and agar was provided by Guangdong Huankai Microbial Sci. & Tech. Co., Ltd. Sponges (made of polyurethane) were provided by local stores, and the ceramic slurry used to prepare ceramic foams was customized at a local ceramic factory and mainly consisted of silicon dioxide, aluminum oxide, potassium oxide, and sodium oxide (the weight ratio was about 36.0 : 10.8 : 1.2 : 1.0).

### 2.2. Preparation of the waterproof sound-absorbing ceramic foams (WSCF)

Sponges with a diameter of 9.8 cm and a thickness of 10 mm were used as the sintering templates for preparing ceramic foams. In particular, different weights of the ceramic slurry (the solid content was about 67.76%), including 330, 360, 390, 420, and 450 g, were absorbed by sponges. Afterwards, the sponges with different ceramic slurry weights were placed in an electric kiln and sintered in three stages. The first stage involved heating to 100 °C at a sintering rate of 100 °C $h^{-1}$ and maintaining insulation for three hours. The second heating stage was up to 350 °C at a sintering rate of 110 °C $h^{-1}$ without insulation. The third heating stage was up to 1230 °C at a sintering rate of 120 °C $h^{-1}$ without insulation. After the sintered samples were cooled down to room temperature, hydrophilic ceramic foams were obtained. The ceramic foams were then immersed in a solution composed of 0.75 g acetic acid, 25.0 g hexane, and 0.5 g PFDTMS. The above mixture was heated at 65 °C for 3 h. After drying at 100 °C for 1 h, desirable waterproof and sound-absorbing ceramic foams were obtained, and the samples

prepared with different ceramic slurry weights are denoted as WSCF1, WSCF2, WSCF3, WSCF4, and WSCF5, respectively.

### 2.3. Determination of ceramic porosity

The ceramic foams were cut into 2 × 2 $cm^2$ samples before the hydrophobic treatment and then placed in an oven at 120 °C for 1 h. After cooling down to room temperature, the weights of the dried samples were measured (denoted as $m$). Afterwards, these samples were suspended in boiling water for 2 h. After cooling down to room temperature, excessive water on the sample surface was wiped off, and the weights of the treated samples were obtained (denoted as $m_1$). Furthermore, the water-absorbed samples were suspended in water, and the added weight, denoted as $m_2$, was recorded. The porosity ($P$) of the ceramic foams was calculated using eqn (1). The calculated porosity is the open porosity (porosity accessible to water).

$$P = \frac{m_1 - m}{m_1 - m_2} \quad (1)$$

### 2.4. Evaluation of the antibacterial performance of the ceramic foams

The antibacterial performance of the ceramic foams was evaluated with respect to the antibacterial rate. First, sterilized ceramic foams with a dimension of 2 × 2 $cm^2$ were immersed in 5 mL *E. coli* or *S. aureus* suspension with a concentration of $10^8$ CFU $mL^{-1}$. After incubation for 3 h at 28 °C, sterile cotton swabs were used to wipe the ceramic surfaces and placed in sterilized tubes with 10 mL Ringer's solution. After ultrasonication for 5 min, 100 μL of the solution was applied evenly on the surface of sterilized nutrient agar and incubated at 37 °C for 8 h. The hydrophilic ceramic foam without fluorination treatment was used as the blank control. The antibacterial rate ($E$) of the sample was determined using eqn (2).

$$E = \frac{N_b - N_c}{N_b} \quad (2)$$

where $E$ is the antibacterial rate of the sample, $N_b$ is the number of bacterial colonies in the blank control group, and $N_c$ is the number of bacterial colonies obtained from the waterproof ceramic foams.

### 2.5. Characterizations

To confirm the compositions of the ceramic foams, X-ray diffraction (XRD, D8-Advance A25, BRUKER) was used to determine the crystalline structures of the ceramic foams. The chemical structures of the ceramic foams were confirmed using Fourier transform infrared spectroscopy (FTIR, Spectrum 100). The morphology and pore structure of the samples were observed using scanning electron microscopy (SEM, NOVA NanoSEM 430), and energy dispersive spectrometer (EDS) mapping was collaboratively implemented to observe the distribution of elements. The pore distributions and average pore sizes of different ceramic foams were determined using Nano Measure software. The water contact angle on the ceramic surface was determined using a contact angle meter (Theta, Biolin), and 5.0 μL of water was used. The sound absorption performance of the ceramic foams was determined by an impedance tube kit using the transfer-function method according to ASTM E1050-12 international standards.

## 3. Results and discussion

### 3.1. Designing of the sound-absorbing ceramic foams with waterproof and antibacterial performance

Multifunctional materials offer attractive solutions to the challenges brought about by urban and technological developments. Nowadays, noise pollution has become serious along with the increasing use of electromechanical equipment, while porous materials with sound-absorbing properties provide an effective approach for noise reduction. However, the hydrophilicity of these materials also results in excessive absorption of water and the proliferation of bacteria, posing potential threats to public safety and health. In this work, a facile strategy was provided to prepare sound-absorbing ceramic foams with waterproof and antibacterial properties. To prepare porous ceramic foams with sound absorption properties, silicon oxide ($SiO_2$) was selected due to its low acoustic impedance for sound absorption,[36] and aluminum oxide ($Al_2O_3$) was utilized to compensate for the mechanical properties of the former.[37] In addition, potassium oxide ($K_2O$) and sodium oxide ($Na_2O$) were used because of their wide application in lowering the sintering temperature.[38] In this multifunctional ceramic system, as demonstrated in Fig. 1, sponges were used as the sintering template, and the amount of ceramic slurry was adjusted to obtain ceramic foams with different pore structures. After the sintering process, the hydrophilicity of the ceramic foams was changed to hydrophobicity by the fluorination treatment of the ceramic surfaces *via* hydrolysis and condensation to achieve sound-absorbing ceramic foams with waterproof and antibacterial properties.

### 3.2. Confirmation of ceramic compositions

In this work, XRD and FTIR characterizations were used to confirm the compositions of the ceramic foams. As demonstrated in Fig. 2a, before fluorination treatment, the XRD pattern displayed diffraction peaks at $2\theta = 22°$, 27°, 40°, and 41° corresponding to the characteristic peaks of $SiO_2$ (JCPDS#46-1441); while the diffraction peaks at $2\theta = 35.5°$, 60°, and 68° were attributed to $Al_2O_3$ (JCPDS#11-0517), the diffraction peak around $2\theta = 37°$ corresponded with $K_2O$ (JCPDS#26-1327), and the diffraction peak at $2\theta = 46°$ was the characteristic peak of $Na_2O$ (JCPDS#23-0528). In addition, the diffraction peak at around $2\theta = 50°$ was mainly ascribed to $Na_2O_2$ derived from the oxidation of $Na_2O$. The above results reveal the compositions of the ceramic foams before fluorination treatment. After modification by PFDTMS, the above diffraction peaks were retained, indicating that the fluorination process had little influence on the crystallinity of the ceramic foams.

Furthermore, the chemical structures of the ceramic foams before and after fluorination treatment were compared using FTIR, as shown in Fig. 2b. Before fluorination treatment, the

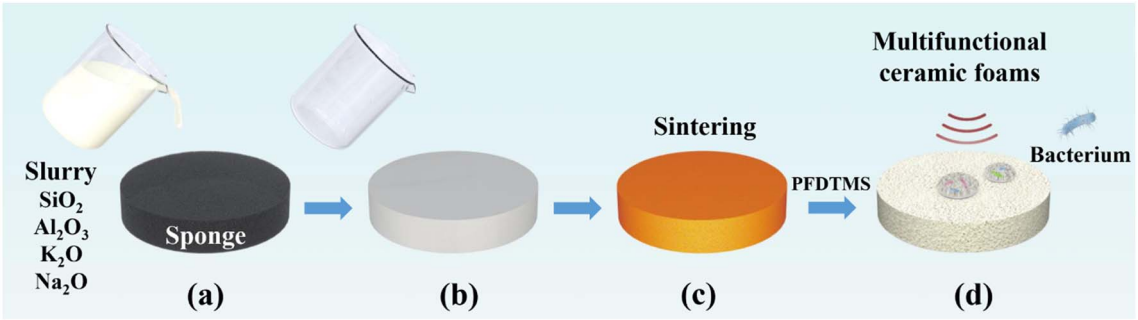


Fig. 1 Preparation route of the ceramic foams with sound-absorbing, waterproof, and antibacterial properties.

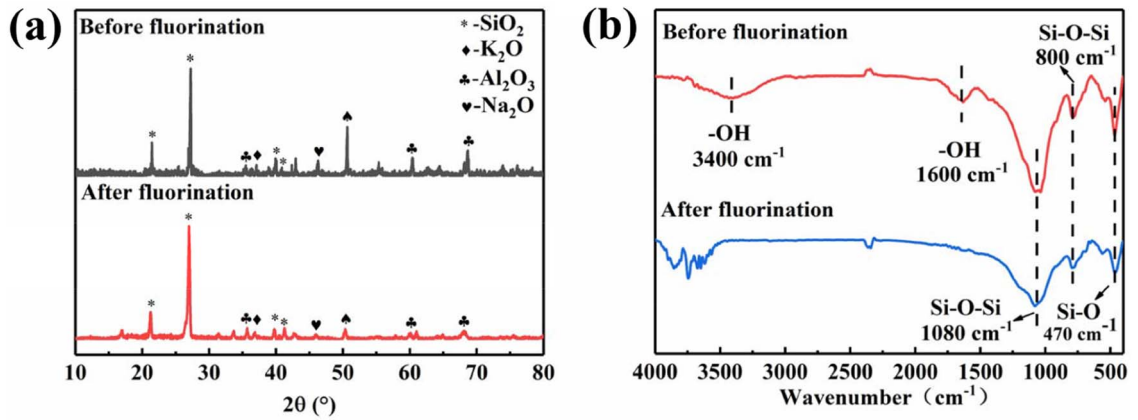


Fig. 2 (a) XRD patterns and (b) FTIR spectra of the ceramic foams.

peak at 470 $cm^{-1}$ attributed to the bending vibration of Si–O and the characteristic peaks at 800 $cm^{-1}$ and 1080 $cm^{-1}$ corresponding to Si–O–Si could be seen.[39,40] In addition, the broad peak at around 3400 $cm^{-1}$ and the peak at 1600 $cm^{-1}$ were ascribed to the presence of hydroxyl groups. After fluorination, the characteristic peak of C–F overlapped with the characteristic peak of Si–O–Si, and the condensation process of PFDTMS consumed the hydroxyl groups, leading to the disappearance of the broad peak. In addition, the confirmation of fluorination treatment was provided by the EDS results (Fig. 4).

### 3.3. Morphology and pore structure of the ceramic foams

In this work, the morphology and pore structure were adjusted by changing the weight of the ceramic slurry. As demonstrated in Fig. 3a–e, millimeter- and micrometer-sized pores were found in all ceramic samples. Due to the compactness of the ceramic components, the pore size visually became smaller along with the increase in the amount of ceramic slurry. This tendency resulted in more complete walls, which might compromise the porosity and weaken the sound-absorbing performance. In addition, the results revealed that the ceramic pore surfaces were rough (Fig. 3f), and the rough pore walls could enhance friction with the sound waves and thus achieve better sound absorption. In addition, creating appropriate roughness is an effective approach to achieving remarkable hydrophobic surfaces. Therefore, the roughness of the ceramic surface would facilitate the achievement of waterproof properties.

In addition, EDS mapping was collaboratively implemented with SEM to investigate the distribution of elements on the ceramic surfaces. As demonstrated in Fig. 4, F, Si, Al, K, Na, C, and O elements were evenly distributed on the ceramic surfaces. Besides, after EDS determination, the Si, Al, K, Na, C, and O element weights on the ceramic surface without fluorination treatment were 45.12%, 10.75%, 3.37%, 0.86%, 3.25%, and 36.65%, respectively, while the F, Si, Al, K, Na, C, and O element weights on the ceramic surface after fluorination treatment were 43.64%, 9.50%, 3.29%, 0.62%, 0.31%, 28.44%, and 14.20%, respectively. Obviously, as for the original ceramic foams, the elemental composition provided above is consistent with the ceramic composition concluded from the XRD analysis (Fig. 2a). After fluorination treatment, coatings derived from the hydrolysis and condensation of PFDTMS were found on the ceramic surface, which is consistent with the FTIR results (Fig. 2b). In addition, such a fluorinated surface is expected to endow the ceramic foams with waterproof and antibacterial properties.

In addition to the elemental distributions, the pore distributions of the ceramic foams were also investigated. As demonstrated in Fig. 5, the ceramic foams exhibited a wide range of pore distributions. As for the ceramic foam prepared with the least weight of the ceramic slurry, the pore size was

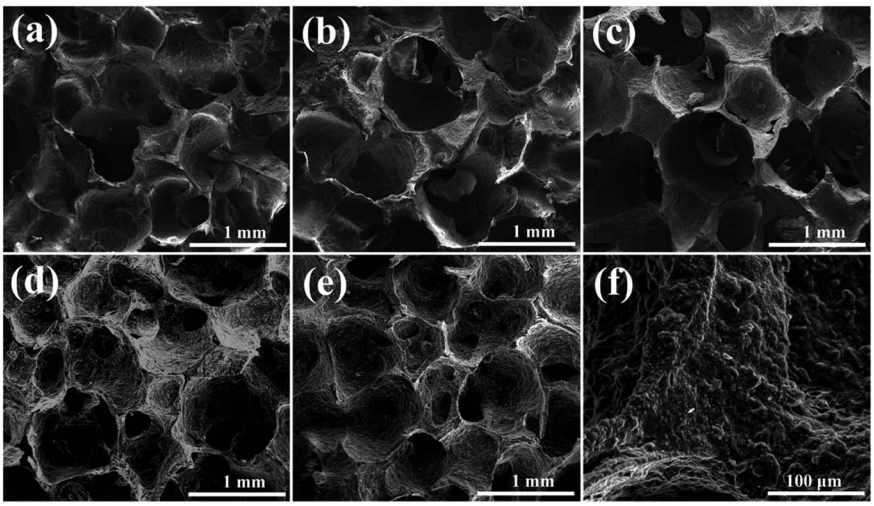


Fig. 3 SEM images of the waterproof sound-absorbing ceramic foams. (a) WSCF1, (b) WSCF2, (c) WSCF3, (d) WSCF4, and (e) WSCF5. Increasing the weight of the ceramic slurry results in a smaller pore size and a complete pore structure. (f) The rough surface of WSCF4.

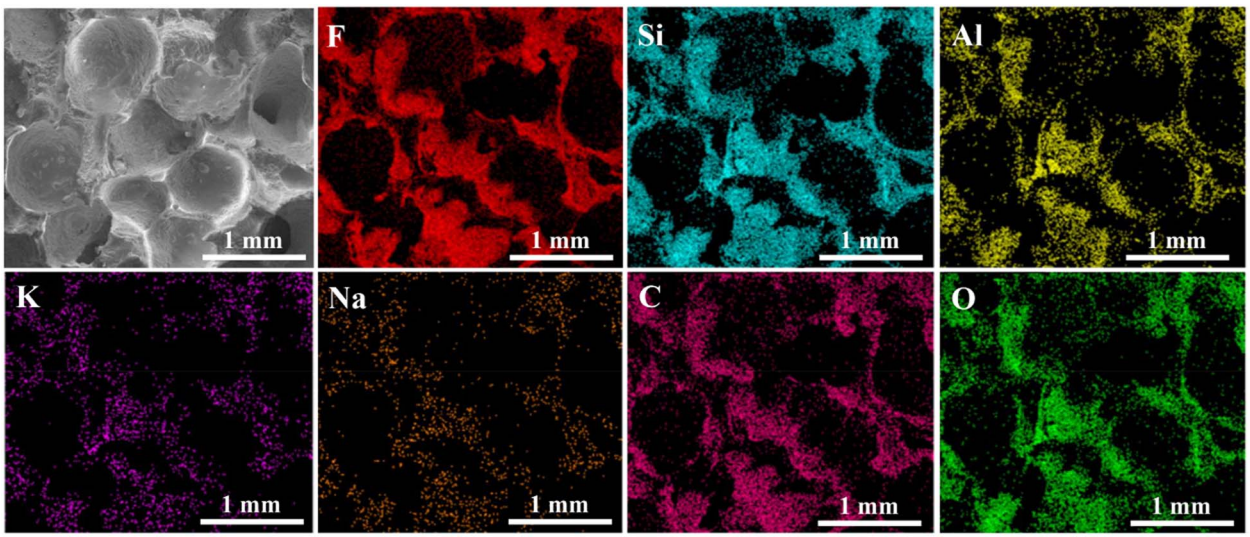


Fig. 4 EDS mapping images showing elemental distributions on the ceramic surfaces.

mainly distributed between 0.25 mm and 0.65 mm, while the pore size of the ceramic foam fabricated with the most weight ranged from 0.15 mm to 0.25 mm. Obviously, the increase in ceramic slurry weight resulted in a decrease in pore size, and the average pore sizes of WSCF1, WSCF2, WSCF3, WSCF4, and WSCF5 were 0.49 mm, 0.45 mm, 0.38 mm, 0.34 mm, and 0.28 mm, respectively. In addition, the influences of pore size on the variations in sound absorption properties and waterproof performance were analyzed.

### 3.4. Sound absorption properties of the ceramic foams

Although the pore distributions of the ceramic foams were analyzed as mentioned above, factors relevant to the sound absorption properties remained unclear. As demonstrated in Fig. 6a, the sound absorption coefficient showed a tendency to increase with the sound frequency, while a further increase in sound frequency gave rise to a decrease in the sound absorption coefficient. The ceramic foams exhibited the highest sound absorption coefficients in the middle-range sound frequency (at about 2500 Hz, the sound absorption coefficient reached 0.92). To further investigate the factors relevant to sound absorption, the noise reduction coefficients (NRC) and average pore sizes of different ceramic foams were summarized and compared, as presented in Fig. 6b. The results reveal that a suitable quantity of the ceramic slurry resulted in a high sound absorption coefficient, whereas excessive ceramic slurry adversely weakened the sound absorption performance. In addition, the increase in the mass of the ceramic slurry resulted in a decrease in pore size due to increasing the compactness of the ceramic components, whereas, the NRC values of the ceramic foams did not completely follow this trend. Specifically, when the average

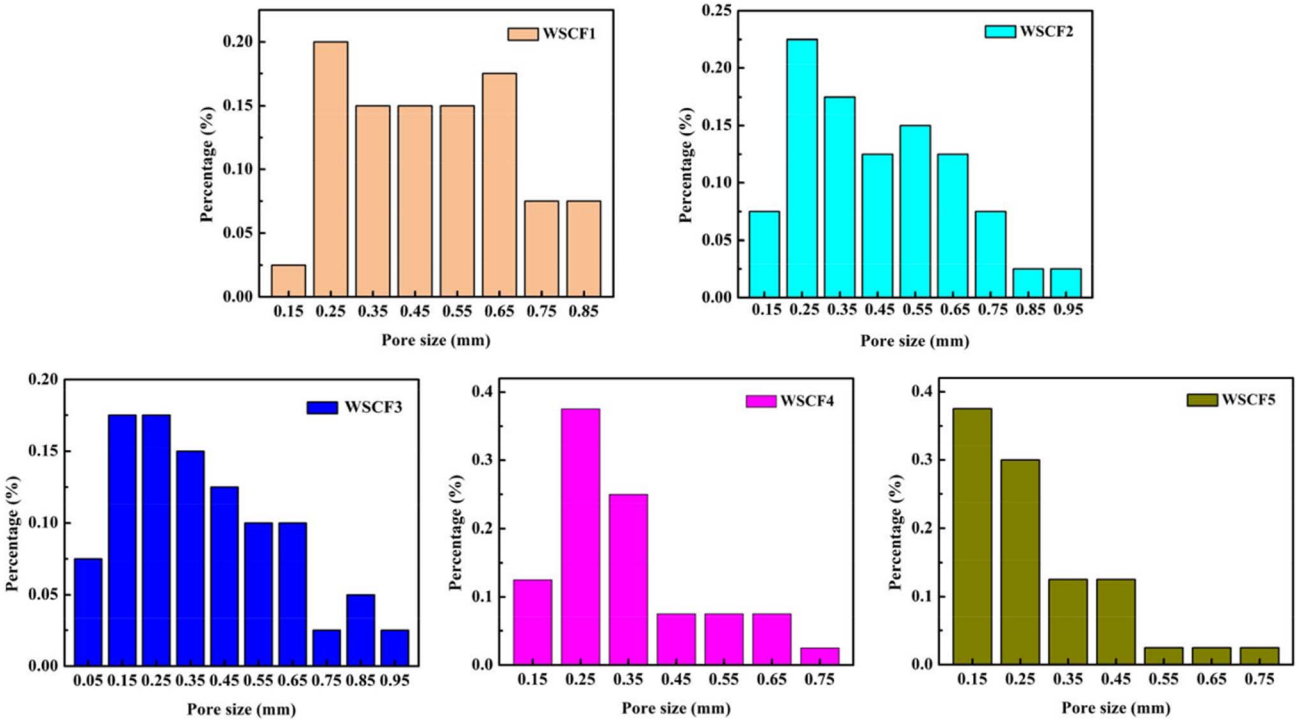


Fig. 5 Pore distributions of different waterproof sound-absorbing ceramic foams.

pore size decreased from 0.49 mm to 0.34 mm, the NRC values increased from 0.314 to 0.46. However, a further decrease in pore size caused a compromise in the sound absorption properties. In fact, the variations in the sound absorption coefficient of this system were mainly influenced by the pore size and porosity. Generally, the pores of ceramic foams and the windows on the pore walls act as resonators to dissipate the energy of the incident sound waves. In addition, the pore sizes are relevant to the resonance effect. The smaller is the pore size, the stronger is the resonance effect. In addition, the decrease in pore size indicated an increase in the surface area of the pore walls, leading to an enhancement in friction and energy loss. However, a high amount of ceramic slurry caused a decrease in the pore size and porosity of the ceramic foams (Fig. S1†). Notably, a decrease in porosity generally makes the transfer of sound waves into the ceramic foams difficult, reducing sound energy loss *via* friction with the pore walls and thus compromising the sound absorption properties. Therefore, the NRC value of WSCF5 decreased to 0.43. In addition, compared to WSCF4, it was found that the sound absorption peak of WSCF5 was shifted to a lower sound frequency. Du *et al.* reported that the sound frequency at the sound absorption peak is proportional to the porosity of ceramic foams.[7] Consequently, the shifting of the sound absorption peak to a lower sound

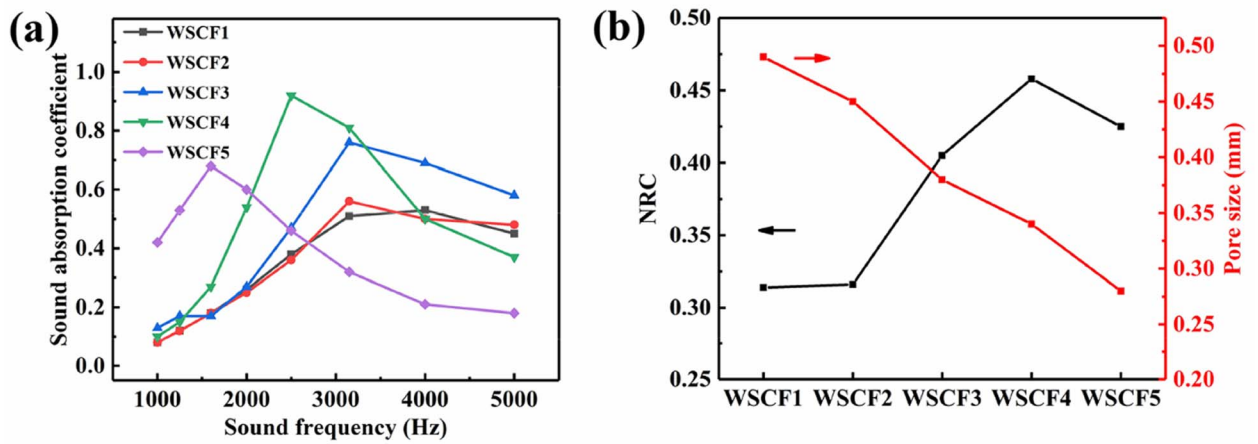


Fig. 6 (a) Sound absorption properties of different ceramic foams. (b) NRC and the average pore sizes of different ceramic foams.

frequency was mainly attributed to the decrease in porosity. As analyzed above, the reduction in pore size facilitated the improvement of sound absorption properties, while this property was also influenced by porosity.

### 3.5. Waterproof properties of the sound-absorbing ceramic foams

Generally, porous ceramics consisting of inorganic materials are highly hydrophilic. It is conceivable that, especially on rainy days, the weight of water absorbed by porous ceramics will exert great pressure on the substrates, and such wet surroundings are conducive to the proliferation of bacteria, thus potentially posing a threat to public safety. Grafting low-surface-tension components on ceramic surfaces is an effective approach to achieving waterproof properties. In this work, on the ceramic foams without fluorination treatment, water droplets were immediately absorbed, indicating the high hydrophilicity of the original samples. Strikingly, after fluorination treatment, the ceramic foams were endowed with waterproof properties. As demonstrated in Fig. 7a, water droplets on the fluorinated ceramic foams exhibited contact angles above 135°. As we know, water contact angles on a smooth surface do not exceed 120°, while hydrophobic materials with a rough surface exhibit contact angles above 120°. As discussed above, the average pore sizes of the ceramic foams decreased with an increase in the weight of the ceramic components, and the low average pore size resulted in high roughness and thus an increase in the water contact angles (Fig. 7a). To further demonstrate the waterproof properties of the ceramic foams, the ceramic foams without and with fluorination treatment were added to a tube with water. As displayed in Fig. 7b, the fluorinated ceramic foam clearly floated on water, and the silver mirror phenomenon was observed on the ceramic surface, while the sample without fluorination sunk into the bottom of the tube due to its hydrophilic property. Therefore, the obtained ceramic foams not only possessed sound-absorbing properties but also exhibited remarkable waterproof performance.

### 3.6. Antibacterial properties of the ceramic foams

As mentioned above, the ceramic foams were waterproof, and such hydrophobic properties are expected to endow the ceramic foams with antibacterial performance. Therefore, the antibacterial performance of the ceramic foams was investigated, and *E. coli* and *S. aureus* were used as the model bacteria. As demonstrated in Fig. 8 and Table S1,† compared with the hydrophilic ceramic foams (blank control), the waterproof ceramic foams exhibited remarkable antibacterial performance. The antibacterial rates of the waterproof ceramic foams against *E. coli* and *S. aureus* were higher than 95%. Remarkably, the antibacterial rates were consistent with the trend of water contact angles, indicating that higher hydrophobicity resulted in greater antibacterial performance. This phenomenon is due to the hydrophobicity-induced reduction in the contact area between the ceramic surfaces and bacterial suspensions, diminishing the residue of bacteria on the ceramic surfaces. Besides, due to the lipophilic property of the fluorine chains, their hydrophobic interactions with the bacteria are conducive to the disruption of the bacterial structure, leading to cell death, which enhances the antibacterial rate to some extent. Therefore, these waterproof sound-absorbing ceramic foams also exhibited remarkable antibacterial performance. Compared with similar waterproof materials,[41,42] the remarkable antibacterial performance achieved in this work indicates that these ceramic foams have the potential to reduce public health risks.

### 3.7. Mechanism of the sound-absorbing, waterproof, and antibacterial performance

As we know, the total sound energy is the sum of reflection, absorption, and transmission. The sound absorption coefficient is generally described as the ratio of the absorbed sound energy to the total incident sound energy. Notably, at a sound frequency of 2500 Hz, the sound absorption coefficient reached 0.92, indicating that most of the incident sound energy was consumed. In terms of the sound absorption process, as demonstrated in Fig. 9, when sound waves strike the porous ceramic foams, air molecules inside the foam vibrate and cause friction with the pore walls, converting sound energy to heat and then dissipating it. In addition, the presence of porosity allows more sound waves to transfer into the ceramic foams and increases the friction with the pore walls. In addition, the resonance effect relevant to pore size and porosity facilitates the improvement of sound absorption. Regarding the waterproof performance, the fluorinated

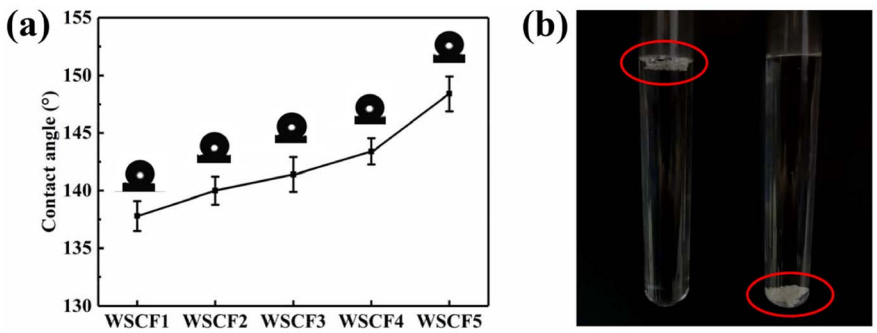


Fig. 7 Waterproof properties of the ceramic foams. (a) Water contact angles on different ceramic surfaces. (b) Waterproof ceramic foams floating on water (left), and hydrophilic ceramic foams sinking to the bottom of the tube (right).

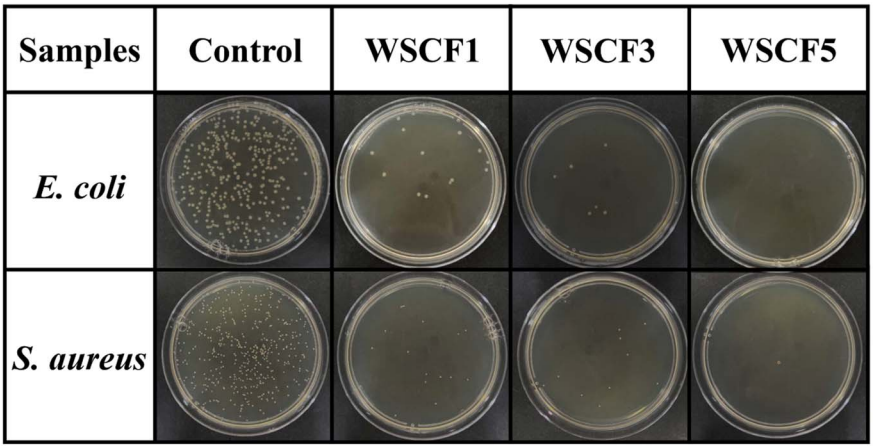


Fig. 8 Antibacterial performance of the waterproof sound-absorbing ceramic foams.

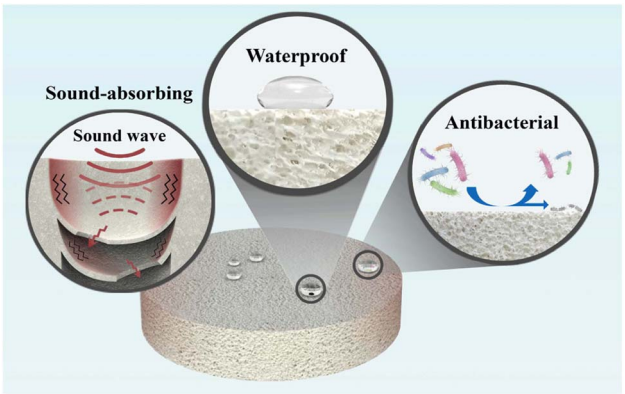


Fig. 9 Mechanism of the multifunctional ceramic foams.

layer lowers the surface energy of the ceramic surfaces, and the roughness of the ceramic surface reduces the contact area with water in collaboration with the air cavities, leading to high water contact angles. In addition, such waterproof properties diminish the residue of bacterial suspension on the ceramic surfaces, enabling the fluorine chains to interact with the bacteria due to the lipophilic properties and thus causing the disruption of the bacterial structure. The above two factors endow this system with remarkable antibacterial performance. Therefore, using a facile strategy, a porous ceramic system with sound-absorbing, waterproof, and antibacterial properties is developed in this work, and such multifunctional ceramic foams have good potential for practical applications.

## 4. Conclusions

In summary, a multifunctional ceramic system was developed using sponges as the sintering template, adjusting the weights of the ceramic slurry to obtain various pore structures, and treating the sintered ceramic foams with PFDTMS *via* hydrolysis and condensation processes, which provide this system with low surface energy. Strikingly, the obtained sound-absorbing ceramic foams not only demonstrated waterproof properties but also exhibited antibacterial characteristics. The ceramic components were confirmed using XRD, FTIR, and EDS characterizations, and the pore structures were observed using SEM analysis. It was found that increasing the weight ratio of the ceramic slurry resulted in a decrease in pore size and porosity, and the low porosity had an adverse influence on the sound absorption properties. In the middle sound frequency, the sound absorption coefficient reached 0.92. In addition, the rough surface along with the low surface energy derived from the fluorination treatment endowed the ceramic surfaces with waterproof properties and thus large water contact angles, due to which the silver mirror phenomenon could be achieved. In addition, the waterproof properties reduced the contact area between the bacterial suspension and the ceramic surface, and the lipophilic fluorine chains were able to disrupt the bacterial structure, which contributed to their remarkable antibacterial performance with antibacterial rates above 95%. In addition, corresponding mechanisms were elucidated. Therefore, this work provides a facile strategy to establish a multifunctional ceramic system; the sound-absorbing, waterproof, and antibacterial performances of the as-prepared foams make them more suitable for practical applications.

## Conflicts of interest

There are no conflicts to declare.

## Acknowledgements

We appreciate the financial support from the Science and Technology Development Fund of the Macao Special Administrative Region (0055/2021/A), the National Natural Science Foundation of China (22108318), and the Guangzhou Science and Technology Plan Project (202201010494).

## Notes and references

1 M. Liang, H. Wu, J. Liu, Y. Shen and G. Wu, *J. Porous Mater.*, 2022, **29**, 869–892.

2 O. Hahad, S. Rajagopalan, J. Lelieveld, M. Sørensen, K. Frenis, A. Daiber, M. Basner, M. Nieuwenhuijsen, R. D. Brook and T. Münzel, *Hypertension*, 2023, **80**, 1375–1383.
3 M. Mir, F. Nasirzadeh, H. Bereznicki, P. Enticott, S. Lee and A. Mills, *Sustainable Cities Soc.*, 2023, **91**, 104470.
4 F. Zou, J. Cucharero, Y. Dong, P. Kangas, Y. Zhu, J. Kaskirinne, G. C. Tewari, T. Hänninen, T. Lokki, H. Li and J. Vapaavuori, *Chem. Eng. J.*, 2023, **462**, 142236.
5 R. Qu, J. Guo, Y. Fang, S. Zhong and X. Zhang, *Int. J. Mech. Sci.*, 2022, **227**, 107426.
6 L. Cao, Q. Fu, Y. Si, B. Ding and J. Yu, *Compos. Commun.*, 2018, **10**, 25–35.
7 Z. Du, D. Yao, Y. Xia, K. Zuo, J. Yin, H. Liang and Y. Zeng, *J. Alloys Compd.*, 2020, **820**, 153067.
8 J. Ning, G. Zhao and X. He, *Phys. Fluids*, 2019, **31**, 037106.
9 J. Lee and J. H. Kim, *Polym. Test.*, 2023, **124**, 108069.
10 F. Ma, C. Wang, Y. Du, Z. Zhu and J. H. Wu, *Mater. Horiz.*, 2022, **9**, 653.
11 H. Kolya, K. Hashitsume and C. W. Kang, *Int. J. Biol. Macromol.*, 2022, **205**, 626–637.
12 P. Filip, T. Sedlacek, P. Peer and M. Juricka, *Polymers*, 2022, **14**, 5049.
13 R. Liu, L. Hou, W. Zhou and Y. Chen, *Appl. Acoust.*, 2020, **170**, 107525.
14 M. J. Jafari, R. F. Madvari and T. Ebadzadeh, *Heliyon*, 2023, **9**, 16428.
15 M. J. Jafari, M. N. Sharak, A. Khavanin, T. Ebadzadeh, M. Fazlali and R. F. Madvari, *Sound Vib.*, 2021, **55**, 117–130.
16 J. H. Chen, P. S. Liu and J. X. Sun, *Ceram. Int.*, 2020, **46**, 22699–22708.
17 H. Zha, W. Yu, J. Li, J. Shi, J. Li, W. Tang, Y. Lin, K. Zhu, J. Cheng and G. Liu, *Silicon*, 2023, **15**, 6631–6653.
18 L. Cao, H. Shan, D. Zong, X. Yu, X. Yin, Y. Si, J. Yu and B. Ding, *Nano Lett.*, 2022, **22**, 1609–1617.
19 M. A. S. Sujon, A. Islam and A. K. Nadimpalli, *Polym. Test.*, 2021, **104**, 107388.
20 C. He, B. Du, J. Ma, X. Xiong, J. Qian, M. Cai and A. Shui, *J. Am. Ceram. Soc.*, 2022, **105**, 3177–3188.
21 V. Bhuvaneswari, B. Devarajan, B. Arulmurugan, R. Mahendran, S. Rajkumar, S. Sharma, K. Mausam, C. Li and E. T. Eldin, *Polymers*, 2022, **14**, 4727.
22 J. Hong and S. W. Cha, *Materials*, 2022, **15**, 2007.
23 J. H. Lin, P. Y. Hsu, C. H. Huang, M. F. Lai, B. C. Shiu and C. W. Lou, *Polymers*, 2022, **14**, 913.
24 S. Bao, M. Zhang, X. Bu, W. Zhang, Z. Jiang and Z. Xie, *ACS Appl. Mater. Interfaces*, 2023, **15**, 13565–13575.
25 X. Zhao, Y. Liu, L. Zhao, A. Yazdkhasti, Y. Mao, A. P. Siciliano, J. Dai, S. Jing, H. Xie, Z. Li, S. He, B. C. Cliford, J. Li, G. S. Chen, E. Q. Wang, A. Desjarlais, D. Saloni, M. Yu, K. Jan, J. Y. Zhu, A. Gong and L. Hu, *Nat. Sustainability*, 2023, **6**, 306–315.
26 K. I. Hegner, C. Hinduja, H. J. Butt and D. Vollmer, *Nano Lett.*, 2023, **23**, 3116–3121.
27 F. Liang, Y. Xu, S. Chen, Y. Zhu, Y. Huang, B. Fei and W. Guo, *ACS Appl. Mater. Interfaces*, 2022, **14**, 56027–56045.
28 H. Yong, Z. Li, X. Huang, K. Wang, Y. Zhou, Q. Li, J. Shi, M. Liu and D. Zhou, *Adv. Mater. Interfaces*, 2022, **9**, 2200435.
29 H. Y. Yong, Z. L. Li, X. B. Huang, K. X. Wang, Y. N. Zhou, Q. X. Li, J. J. Shi, M. Liu and D. Z. Zhou, *Adv. Mater. Interfaces*, 2022, **9**, 2200435.
30 X. Xie, X. Chen, P. A. Levkin and W. Feng, *Adv. Mater.*, 2022, **34**, 22036.
31 W. Huang, J. Huang, Z. Guo and W. Liu, *Adv. Colloid Interface Sci.*, 2022, **304**, 102658.
32 X. Zhong, L. Lv, H. Hu, X. Jiang and H. Fu, *Chem. Eng. J.*, 2020, **382**, 123042.
33 R. N. Wenzel, *Ind. Eng. Chem.*, 1936, **28**, 988–999.
34 J. Lin, X. Chen, C. Chen, J. Hu, C. Zhou, X. Cai, W. Wang, C. Zheng, P. Zhang, J. Cheng and Z. Guo, *ACS Appl. Mater. Interfaces*, 2018, **10**, 6124–6136.
35 J. Lin, X. Cai, Z. Liu, N. Liu, M. Xie, B. Zhou, H. Wang and Z. Guo, *Adv. Funct. Mater.*, 2020, **30**, 2000398.
36 M. Kadota, Y. Ishii and S. Tanaka, *Jpn. J. Appl. Phys.*, 2021, **60**, 11.
37 H. J. Conrad, W. J. Seong and I. J. Pesun, *J. Prosthet. Dent.*, 2007, **98**, 389–404.
38 J. Partyka, *Ceram. Int.*, 2015, **41**, 9337–9343.
39 X. Zhong, H. Hu and H. Fu, *ACS Appl. Mater. Interfaces*, 2018, **10**, 25697–25705.
40 X. Zhong, H. Wen, R. Zeng, H. Deng, G. Su, H. Zhou and X. Zhou, *Ind. Crops Prod.*, 2022, **188**, 115716.
41 Y. X. Chen, K. M. Klima, H. J. H. Brouwers and Q. Yu, *Composites, Part B*, 2022, **242**, 110048.
42 X. Lv, W. Cao, M. Yio, J. Lu and C. S. Poon, *Chem. Eng. J.*, 2023, **478**, 147390.